THE UNIVERSITY of EDINBURGH

Edinburgh Research Explorer

Atmospheric HCFC-22, HFC-125, and HFC-152a at Cape Point, South Africa

1 # HCFCs and HFCs in the atmosphere at Cape Point,

2 # South Africa

3 Brett Kuyper[1], Daniel Say[2], Casper Labuschagne[3], Timothy Lesch[1], Warren R. Joubert[3], Damien

4 Martin[2], Dickon Young[2], M. Anwar H. Khan[2], Matthew Rigby[2], Anita L. Ganesan[4], Mark F.

5 Lunt[5], Alistair J. Manning[2,6], Simon O'Doherty[2], Michael T. Davies-Coleman[1], Dudley E.

6 Shallcross[1,2]

7 [1]Department of Chemistry, University of the Western Cape, Bellville 7535, South Africa

8 [2]Atmospheric Chemistry Research Group, School of Chemistry, University of Bristol, Bristol,
9 BS8 1TS, United Kingdom

10 [3]Climate and Environmental Research and Monitoring, South African Weather Service,
11 Stellenbosch 7600, South Africa

12 [4]School of Geographical Sciences, University of Bristol, Bristol, BS8 1SS, United Kingdom

13 [5]School of Geosciences, University of Edinburgh, Edinburgh, EH9 3JW, United Kingdom

14 [6]Hadley Centre, The Met Office, Exeter, EX1 3PB, United Kingdom

15
16
17

18

ABSTRACT

20

21One hydrochlorofluorocarbon and two hydrofluorocarbons (HCFC-22, HFC-125, HFC-152a)
22were measured in air samples at the Cape Point observatory (CPT), South Africa during 2017.
23These data represent the first such atmospheric measurements of these compounds from south
24western South Africa. Our results indicate Cape Town to be the dominant source of the
25halocarbon pollution events observed at CPT. Baseline atmospheric growth rates were estimated
26to be 8.36 ppt yr^{-1}, 4.10 ppt yr^{-1} and 0.71 ppt yr^{-1} for HCFC-22, HFC-125 and HFC-152a,
27respectively. The CPT measurements were combined with an inverse model to investigate the
28possibility of estimating emissions for South Africa. The results exhibited some dependency on
29the choice of prior – this could be reduced with further measurements, particularly in the winter
30months during which the instrument was down, but which coincided with a maximum in the
31sensitivity of CPT to terrestrial sources. At 3.6 (1.3 – 8.7) Gg yr^{-1} for HCFC-22, 1.6 (0.8 – 2.6)
32Gg yr^{-1} for HFC-125, and 0.13 (0.10 – 0.19) Gg yr^{-1} for HFC-152a, the current contribution of
33South Africa to the global emissions of these gases is relatively minor. Further measurements
34could provide a useful means to verify progress made by South Africa towards its Montreal
35Protocol commitments.

36

37 Keywords: HFC, HCFC, South Africa, climate, greenhouse gases, ozone depleting
38substances, emissions

INTRODUCTION

40 The phasing-out of the industrial production of chlorofluorocarbons (CFCs), as a direct
41consequence of the Montreal Protocol, has led to an increase in the production and use of
42hydrochlorofluorocarbons (HCFCs) and hydrofluorocarbons (HFCs) as substitutes. Commonly
43used as refrigerants in air conditioners and in the production of insulating foams. HCFCs and

44HFCs also find widespread applications as solvents used in lubricants, coatings and cleaning

45fluids. The presence of a reactive hydrogen atom in the molecular structures of HCFCs and

46HFCs results in these compounds being more susceptible to attack and degradation in the

47troposphere through reaction with hydroxyl radicals (OH).[1,2] HFCs have zero Ozone Depletion

48Potentials (ODP) as they contain no chlorine or bromine atoms and, despite the presence of

49chlorine in HCFCs these compounds have lower ODPs than the CFCs they replace.[3] Conversely,

50HCFCs and HFCs both have an immediate and significant effect on the Earth's climate due to

51their high global warming potentials (GWP).[4,5] Given their non-negligible ODPs and high

52GWPs,[6] the industrial production of HCFCs has been controlled under the Montreal Protocol and

53its amendments since 1992, and owing to their high GWPs, the production of HFCs will now be

54regulated following the Kigali amendment to the Protocol.[7,8]

55 HCFC-22 ($CHClF_2$), which has a tropospheric lifetime of 11.9 years[9], was introduced in the

56early 1990s as a replacement for CFCs and is the most abundant HCFC in the atmosphere[10]. The

57GWP of HCFC-22 is 1760 integrated over a 100-yr time horizon (GWP_{100})[9] and its ODP is

580.055.[11] The principal removal process for this compound from the atmosphere is reaction with

59OH (k_{OH} = 5.0 $\times$ 10^{-15} cm^3 molecule^{-1} s^{-1} at 298 K).[12] Following a maximum global mean growth

60rate in 2007 of 8.2 ppt yr^{-1}, the rate of growth had decreased by 2015 to 3.7 ppt yr^{-1} (-54%).[11] The

61emissions of HCFC-22 have now stabilized at approximately 370 Gg yr^{-1} (2016) due to the

62freezing of HCFC production and consumption for dispersive (emitted to the atmosphere) uses in

63developing countries.[9,13] Production is limited to existing chemical plants and no increase in

64production is permitted under the Montreal Protocol guidelines. Currently, the main source of

65emission of HCFC-22 into the atmosphere is a result of leakage from refrigeration equipment

66either during use, servicing or final disposal, rather than from the chemical plants in which it is

67produced.[14] Traditionally, emissions from leakage and servicing were thought to be relatively

68constant throughout the year.[15] However, more recent studies have suggested that there is

69significant seasonality in the emission rates of HCFC-22. Xiang et al.[16] estimated that emissions

70of HCFC-22 were over twice as large during summer months, compared to the winter. While this

71seasonal cycle is observed globally, the magnitude is larger in the northern hemisphere.[16] The

72authors proposed that the increased usage rates and ambient temperatures (resulting in greater

73charge pressures and hence greater leakage) generally associated with summer months as

74potential reasons for the observed seasonality.

75 HFC-125 (CF_3CHF_2) is the third most abundant HFC and currently makes the third largest

76contribution of the HFCs to atmospheric radiative forcing value with a GWP_{100} of 3500.[9,17,18] The

77atmospheric lifetime of HFC-125 is estimated to be 31 years[9] and this trace gas is removed from

78the atmosphere by reaction with OH resulting in *inter alia* carbonyl fluoride and

79trifluoromethanol degradation products. In 2015, the global average mixing ratio of HFC-125

80was 18.4 ppt in the lower troposphere with an estimated growth of 2.3% per annum for the

81period of 1995-2015.[11] HFC-125 is almost exclusively used in blends with HFC-134a, HFC-143a

82and HFC-32. Common examples of these blends include R-410A (50% by wt. HFC-125, 50% by

83wt. HFC-32) and R-407C (52% by wt. HFC-134a, 25% by wt. HFC-125, 23% by wt. HFC-32).

84Both blends were designed as replacements for HCFC-22, in applications including domestic air-

85conditioning and commercial refrigeration. Commercial refrigeration systems, in particular, are

86notorious for their high leakage rates, with as much as 30% charge loss per year.[19] The rapid

87increase in global HFC-125 mixing ratios is well documented (e.g. Lunt et al.[20]; Li et al.[21]).

88 HFC-152a (CH_3CHF_2) has a relatively small GWP of 138[17] and a significantly shorter

89atmospheric lifetime of approximately 1.5 years[9,22], compared with other HFCs. Consequently,

90HFC-152a is often used as a replacement for CFCs, various HCFCs and HFC-134a in technical

91aerosol applications, foam blowing and mobile air-conditioners. A rapid accumulation of HFC-

92152a in the atmosphere up to 2012, with increases of 8.9 ppt (1992 – 2012) and 3.7 ppt (1998 –

932012) for the Northern and Southern Hemispheres respectively, were reported.[22] However, the

94global mean mixing ratio has since stabilized, with a global mean growth rate post-2012 that

95does not differ significantly from 0 ppt yr^{-1} (-0.06 ± 0.05 ppt yr^{-1})[22]. Global emissions were

96estimated to be 52.5 ± 20.1 Gg yr^{-1} in 2014.[22]

97 The production and consumption of HCFCs is controlled by amendments to the Montreal

98Protocol. Specifically, the HCFC Phase-out Management Plan (HPMP) seeks to define targets

99for the reduction of HCFC consumption in developing countries such as South Africa. Under

100stage two of the HPMP, these countries agreed to freeze their consumption of HCFCs by 2013,

101followed by a 10% reduction by 2016. A complete ban on the production and consumption of

102HCFCs for dispersive applications is planned for 2030.[23] South Africa is expected to ratify the

103Kigali Amendment to the Montreal Protocol, which sets out phase-down targets for HFCs.

104However, developing countries will not be required to make their first reductions until 2040.

105 Given the greater population and industrialization in the Northern Hemisphere, a North-South

106interhemispheric gradient has been established for all of these compounds.[11,22] The number of *in-*

107*situ* measurements of HCFCs and HFCs available from Northern Hemispheric sites exceeds

108those available from the Southern Hemisphere. Continuous measurements of three CFCs (CFC-

10911, CFC-12 and CFC-113) and TCE have been made at the Cape Point Global Atmospheric

110Watch Station, South Africa over the period 1979-2015.[24] Extension of the range of tropospheric

111HCFC and HFC concentrations measured at sites in the Southern Hemisphere is required for

112more robust constraints on global, southern-hemispheric and regional emissions estimates. In this

113study, we report the 2017 time series of atmospheric mixing ratios of HCFC-22, HFC-125 and

114HFC-152a at Cape Point, South Africa. We consider variations in the mixing ratios of each gas

115with respect to various meteorological parameters (e.g. wind speed and direction) and use an

116inverse model to provide the first documented top down emissions estimates of HCFC-22, HFC-

117125 and HFC-152a for South Africa.

118

119METHODS

120Global Atmospheric Watch Monitoring station

121 The South African Weather Service manage and maintain the Global Atmospheric Watch

122(GAW) monitoring station at Cape Point (34.5º S, 18.2º E) situated approximately 60 km south

123of the City of Cape Town (population ~4 million). The station is situated on an elevated

124peninsula (230 m above sea level) extending out into the south Atlantic (Figure 1). The local

125seasonal synoptic patterns around Cape Town results in predominantly clean marine air arriving

126at Cape Point during austral summer and occasionally anthropogenically modified air arriving

127during austral winter.[24,25] The differing air mass sources are driven by South Atlantic High

128Pressure (SAHP) system which occupies a latitudinal position roughly in line with Cape Town

129during summer, driving strong south-easterly winds, drawing air from deep in the south Atlantic,

130towards Cape Point.[25–27] The SAHP system retreats to the north during austral winter, thus

131allowing transient low-pressure systems to impact Cape Town and Cape Point.[25–28]

132

133
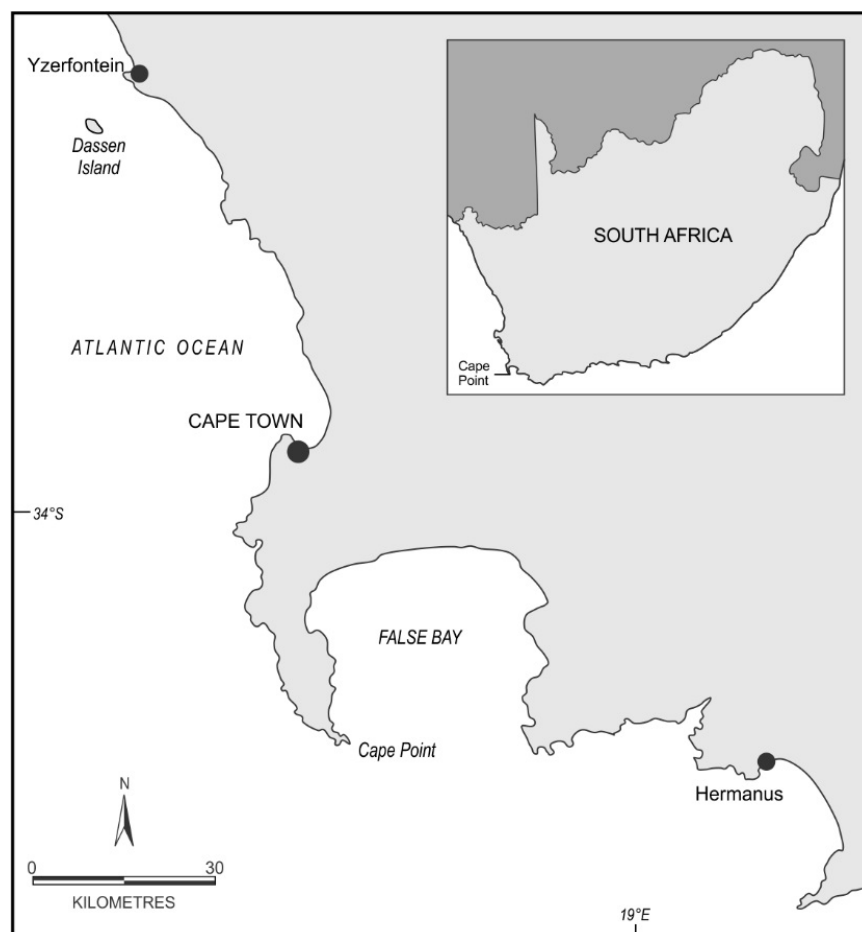
Figure 1. Cape Point and the GAW monitoring station in relation to Cape Town and the south Atlantic Ocean.

136

Cape Point Gas Chromatograph-Mass Spectrometer

An Agilent gas chromatograph-mass spectrometer (GC-MS, 6890/5973N) with a custom-built adsorption/desorption system (ADS) was used to measure HCFC and HFC mixing ratios in the atmosphere at Cape Point.[29] Air samples for analysis were drawn through a 15 m x ¼" OD stainless steel sampling from above the laboratory at ~17 l min^{-1} by a diaphragm pump (GAST, Miniature Diaphragm Pump 22D). Samples and standards were autonomously pre-concentrated

143on a triple bed microtrap (3 mg Carbotrap B; 5 mg Carboxen 1003; 4 mg Carboxen 1000) at -50

144ºC in the ADS.[30,31] Following pre-concentration on the microtrap, samples or standards were

145heated to 240 ºC and injected directly on to the column (CP Sil-5, 100m x 0.32 mm x 5 μm) at

146240 ºC. Separation of the injected sample was achieved with a helium carrier flow (1.8 ml min^{-1})

147and temperature programme with an initial isothermal period (30 ºC, 12 min) and temperature

148gradient (10 ºC min^{-1} to 150 ºC).

149 A short-term working standard, filled at Cape Point under baseline conditions, was analysed

150alternately to each air sample, to account for instrument drift. Calibrated mixing ratios were

151assigned to short-term working standards from an external long-term working standard tank

152which was calibrated using the Advanced Global Atmospheric Gases Experiment (AGAGE)

153Medusa GC-MS at Mace Head.[32,33] The procedure provided a direct comparison of the short-term

154working standard with the relevant Scripps Institute of Oceanography (SIO) primary calibration

155scales.[32] The calibration of the long-term working standard (filled at Mace Head) had mixing

156ratio values assigned from SIO-05 (HCFC-22 and HFC-152a) and SIO-14 (HFC-125). A

157complete description of the ADS-GC-MS system and set up can be found in Simmonds et al.[29]

158

159Baseline classification algorithm

160 A statistical method based on the Advanced Global Atmospheric Gases Experiment (AGAGE)

161pollution algorithm was developed to identify baseline samples within long-lived trace gas mole

162fraction datasets. A full description can be found in the SI and the appendix to O'Doherty et al.[34]

163and Simmonds et al.[22]. In brief, a second order polynomial is fitted to the daily minima over a

164121-day window. The polynomial was subtracted from each data point in the window, creating a

165matrix of distances. Measurements that were larger than 3 times the median of the distances were

166marked as 'polluted'. This was repeated all the 'polluted' marked data removed. Measurements

167between 2-3 times the median were marked as 'possibly polluted'. In the final step 'possibly

168polluted' measurements were tested for adjacency with 'polluted' measurements.

169

170Atmospheric dispersion modelling using NAME

171 The U.K. Meteorological (Met.) Office's Lagrangian atmospheric dispersion model, NAME

172(Numerical Atmospheric dispersion Modelling Environment), was used to simulate 30-day back-

173trajectories for each atmospheric measurement.[35] The NAME model was driven by

174meteorological fields derived from the operational analysis of the U.K. Met. Office Numerical

175Weather Prediction model, the Unified Model (UM), at an approximate horizontal resolution of

17617 km in 2017 (reduced to ~12 km from 11th July 2017). The model domain spanned from 64° S

177to 4.3° N, and from 50° W to 87.3° E, covering southern Africa and the south Atlantic (Figure 2).

178Particles were released into the model domain from randomly generated points on a 20 m

179vertical line, centred on the Cape Point inlet (30 m above ground level) at a rate of 333 particles

180min^{-1}. All particles were assumed to be inert throughout the length of each 30-day simulation.

181Given the long lifetimes of the HCFC and HFCs studied here, this assumption can be made with

182very little loss of accuracy. At the edges of the NAME model domain, the 3-dimensional location

183and time at which each particle left the domain was recorded to provide sensitivity to mole

184fraction boundary conditions.
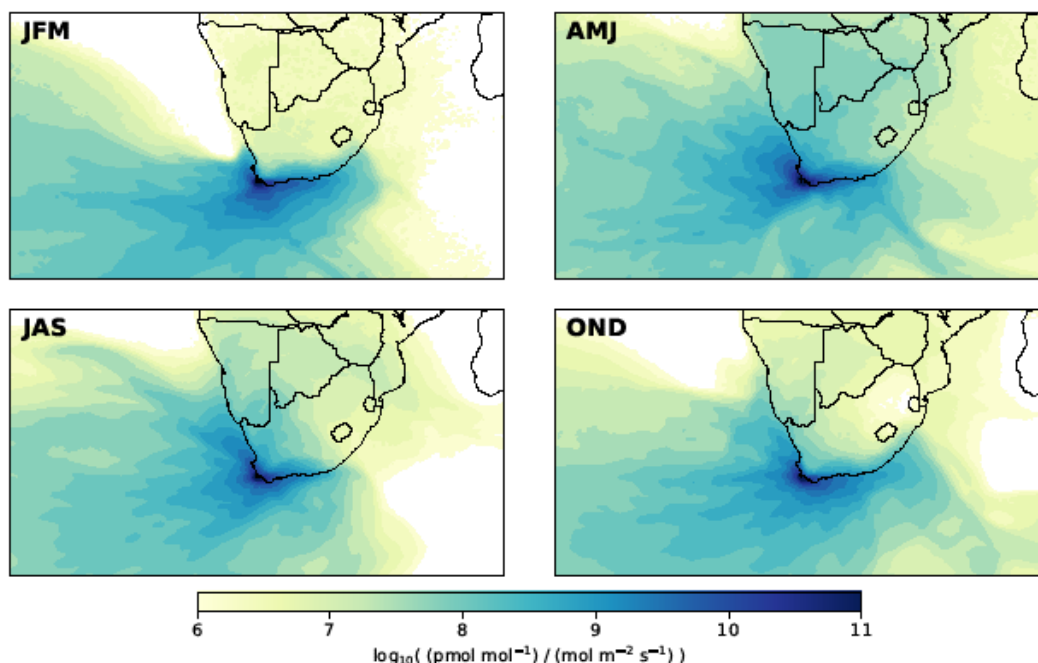
185

186Figure 2: Mean 2017 quarterly air history footprints at Cape Point using the NAME model.

187

188Estimating emissions using a hierarchical trans-dimensional Bayesian 189framework

190 A hierarchical trans-dimensional Bayesian framework was used to estimate South Africa's 191halocarbon emissions using the atmospheric measurements made at Cape Point. A full 192description of the inverse method can be found in Lunt et al.[36] The hierarchical treatment of 193uncertainties is described by Ganesan et al.[37] This inverse method has been used to estimate 194halocarbon emissions from other regions.[38,39] In short, the inverse approach attempts to solve for 195a parameters vector, x (including the flux grid and boundary conditions), using a set of 196atmospheric observations, y. The system starts from an *a priori* flux field, x_{ap}, which is adjusted 197using the atmospheric measurements in order to estimate the posterior flux field, x, in

198conjunction with a linear model, **H**. **H** is a Jacobian matrix of sensitivities which describes the

199relationship between changes in atmospheric mixing ratio and the parameters vector, x. In a

200traditional Bayesian set-up, uncertainty in the *a priori* emissions (x_{ap}) and model-measurement

201mismatch (ε) are defined prior to the inversion. Hence, they are based on a subjective decision by

202the investigator. However, the choice of uncertainties has been shown to significantly influence

203the posterior solution. The hierarchical framework attempts to reduce the influence of this

204subjectivity by introducing hyper-parameters which define the uncertainties within these

205uncertainties.

206 A reversible-jump Markov Chain Monte Carlo algorithm (rj-MCMC) was used to estimate the

207posterior solution.[36] For each species, the rj-MCMC algorithm was run for a chain length of

208400,000. The first 100,000 iterations were discarded to ensure that the system had no knowledge

209of the initial state. The remaining 400,000 iterations were then thinned via sub-sampling of every

210100th iteration, resulting in 4000 samples, which were used to form the posterior PDFs. The

211emission estimates discussed in the following sections represent the means of these PDFs, with

212the corresponding uncertainty estimated by the 95th percentile confidence interval of the same

213PDFs.

214

215 *A priori* emissions

216 Little detailed information is available for South Africa's halocarbon emissions. Therefore, *a*

217*priori* emissions were constructed from a variety of sources which together represent the existing

218state of knowledge. In the absence of emissions data, HCFC-22 a priori emissions were

219estimated using consumption data from South Africa's most recent HPMP report, which was

220estimated at 3.16 Gg yr^{-1} in 2009. In general, consumption is not a good approximation for

221emissions magnitudes (as, for this gas, emissions are likely dominated by release from the bank).

222However, as no estimates exist for South African emissions, we use consumption statistics as a

223proxy for emissions, but with a very large uncertainty (see below), on the assumption that they

224are of a similar order of magnitude to emissions. For HFC-125 and HFC-152a, emissions were

225taken from the EDGAR v4.2 emissions inventory, which reports gridded emissions data up to

2262009. For all three gases, the a priori emissions total was distributed across the inverse model

227domain using the National Oceanic and Atmospheric Administration (NOAA) DMSP-OLS

228(Defence Meteorological Program - Operational Line-Scan System) satellite night-light data.

229These data are available at the increment of 30 arc second from

230https://ngdc.noaa.gov/eog/data/web_data/v4composites/. Night-lights have been shown to

231correlate with population density,[40] and hence this distribution is expected to be roughly

232representative of the sources of all three domestically consumed halocarbons. In each instance,

233the *a priori* emissions were given a 100% uncertainty, with the magnitude of this uncertainty

234further described by a uniform PDF with upper and lower bounds of 50% and 400% respectively.

235This PDF was explored within the inversion.

236

237Boundary conditions

238 We incorporate boundary conditions to account for emissions from outside of the model

239domain. Uniform mixing ratio 'curtains' were estimated using output from the AGAGE 12-box

240model; an extension of the work by Rigby et al.[41] The 12-box model resolves baseline mixing

241ratios for four semi-hemispheres. For each month in which measurements were obtained, the

242simulated mixing ratio from latitude bands 0-30° N, 0-30° S and 30-90° S were assigned to the

243North, East and West and South boundaries of the model domain respectively. The sensitivity of 244each measurement to the boundary conditions was estimated by mapping the exit locations of 245particles from the model domain for each measurement. The *a priori* boundary conditions were 246adjusted within the inversion.

247

248RESULTS AND DISCUSSION

249Cape Point measurements and observations

250 The baseline mixing ratios of one hydrochlorofluorocarbon and two hydrofluorocarbons 251(HCFC-22, HFC-125, HFC-152a) were determined from measurements made at the Cape Point 252Global Atmospheric Watch Station in 2017. The measurements were clustered along a baseline 253for the three species with occasional elevated data points (Figure 3). The mean mixing ratios 254observed at Cape Point were: HCFC-22: 237.80 ± 12.31 ppt; HFC-125: 22.47 ± 1.78 ppt and 255HFC-152a: 6.44 ± 5.32 ppt. The Cape Point HCFC-22 and HFC-125 mixing ratios increased 256throughout the year, in contrast with HFC-152a which displayed a small seasonal cycle. The 257increase through the year for HCFC-22 and HFC-125 was particularly noticeable for the last 258three months of 2017. Variability within the HCFC-22 and HFC-125 mixing ratios, particularly 259in the early part of the year, were observed. Changes in wind direction, and therefore source 260contributions, likely contributed significantly to the observed variability.

261 The HFC-152a mixing ratio increased between February and May, which continued in June. 262Following the winter maximum, the HFC-152a mixing ratios decreased through the latter half of 263the year. A lower rate of growth in the HFC-152a mixing ratios, compared with HCFC-22 and 264HFC-125, was observed over the year. The HFC-152a mixing ratios displayed a maximum in

265austral winter and minima in January and December. The seasonal cycle observed in the HFC-

266152a mixing ratios was likely driven by the winter minimum OH concentration. The shorter

267atmospheric life of HFC-152a compared with HCFC-22 and HFC-125 highlights the sensitivity

268of this compound to reaction with OH, resulting in the observed seasonal cycle.

269
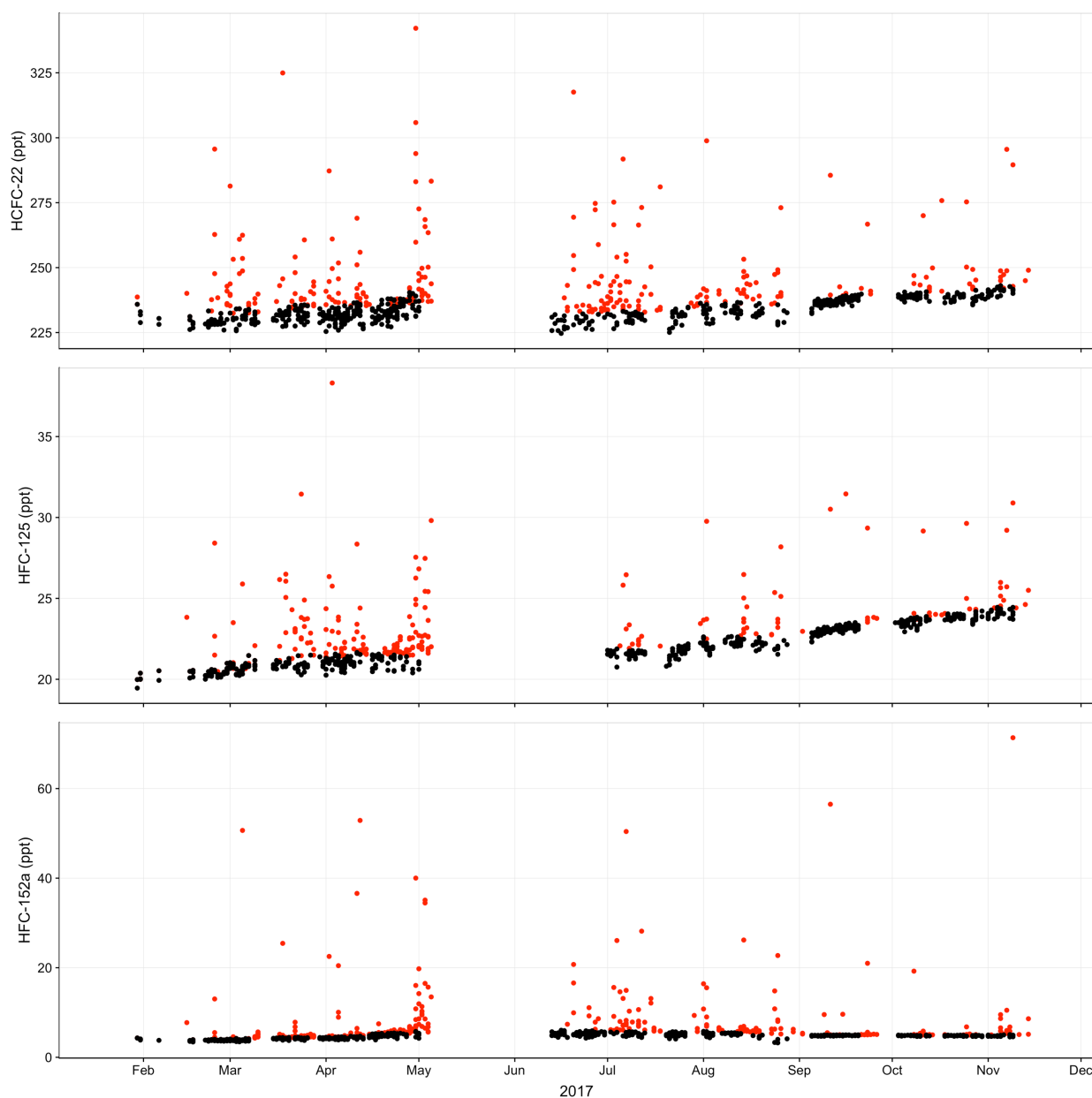
270**Figure 3. Time series of the HCFC and HFCs measured in the atmosphere at Cape Point.**

271The gaps in the data represents instrument down time. Black points highlight the baseline

272measurements while red denote air from polluted sources.

273 The baselines within the Cape Point HCFC and HFC datasets were identified using the adapted

274AGAGE algorithm described in the Baseline Classification Algorithm in the Supplementary

275Information.[22,34] The algorithm relied on the iterative fitting of a second order quadratic function

276to the daily minima over a 121-day window.[22,34] An analysis of the 'polluted' points identified by

277the pollution algorithm, suggests that these were specific intrusions of anthropogenically

278modified air arriving at Cape Point. The pollution events at Cape Point strongly suggest the

279prevalence of local source of all three of these compounds. Baseline mixing ratios at Cape Point

280for HCFC-22, HFC-125 and HFC-152a grew by 8.36 ppt yr^{-1}, 4.10 ppt yr^{-1} and 0.71 ppt yr^{-1},

281respectively, during the 2017 data acquisition window. The mean baseline mixing ratios from

282Cape Point were 233.50 ± 4.0 ppt, 21.95 ± 1.2 ppt, and 4.69 ± 0.5 ppt for HCFC-22, HFC-125

283and HFC-152a, respectively. The baseline growth rates and mean mixing ratios reported here are

284in line with previous studies of the concentrations of these compounds in the atmosphere at

285another Southern Hemisphere site, Cape Grim (e.g. Simmonds et al.[13,22]). The baseline mixing

286ratios reported here were similar to reported global averages.[11,22] Any differences could be

287attributed to either the Southern Hemisphere location where these measurements were made, or

288the existence of additional, as yet unidentified, anthropogenic sources of these compounds in the

289region.

290 The measurements made at Cape Point imply that the HCFC and HFCs share a common

291anthropogenic source situated in the wider City of Cape Town metropole. A bivariate analysis of

292the HCFC and HFC measurements from Cape Point indicate a good agreement with a dominant

293source to the north-east, most probably from stationary air conditioning units (Figure 4). HCFC-

29422 and HFC-125 appear to have greater spread of sources, based on the air sampled at Cape

295Point, whereas HFC-152a seems to have a single dominant source located immediately to the

296north of Cape Point, as shown in the bivariate plots (Figure 4c). Interestingly, the pollution

297marked HCFC and HFC measurements showed only marginal relationships (r^2 < 0.5) with

298known anthropogenic markers such as carbon monoxide and [222]Rn. The lack of relationship

299between HCFC and HFC mixing ratios and anthropogenic markers observed here is consistent

300with previous studies of this kind (e.g. Rivett et al.[42,43], Mead et al.[44], Khan et al.[45]). The HCFC-

30122 and HFC-125 relationship displayed weak commonality in the pollution marked air, to an r^2 of

3020.37.

303
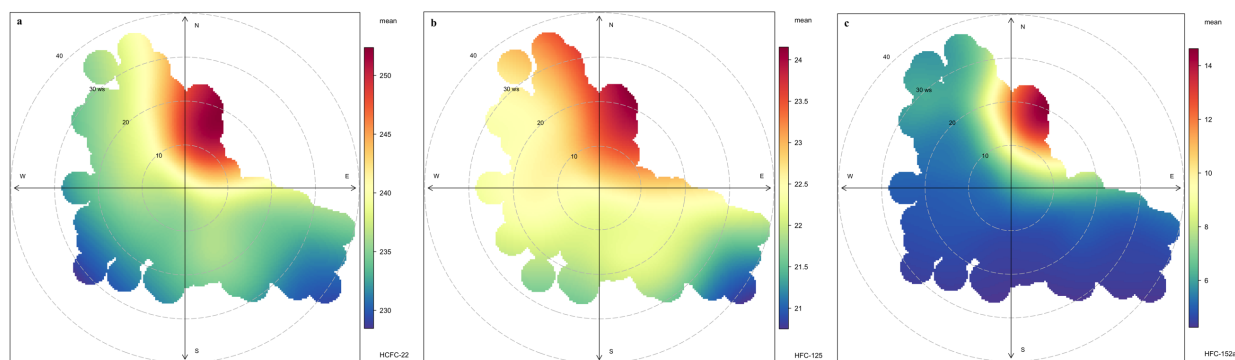
304**Figure 4. Bivariate plots for HCFC and HFC measurements at Cape Point.** HCFC and HFC

305mixing ratio displayed as a function of wind speed and direction for a. HCFC-22, b. HFC-125,

306and c. HFC-152a.

307

308**Estimation of South African HCFC-22, HFC-125 and HFC-152a emissions**

309**using an inverse model**

310 When used in conjunction with an inverse model, long-term atmospheric measurements from
311 the Cape Point observatory could potentially be used to estimate South Africa's halocarbon
312 emissions. In the absence of an annual bottom-up inventory, which South Africa is not currently
313 required to submit, these top-down estimates could provide a useful means by which to track
314 emissions from Africa's second largest economy. To explore this potential, we estimate South
315 Africa's emissions of HCFC-22, HFC-125 and HFC-152a in 2017 using the hierarchical trans-
316 dimensional Bayesian framework described in the Methods section. The estimates presented in
317 the following discussion are based on the mean value of each posterior probability density
318 function (PDF), with an estimation of the corresponding uncertainty taken to be the 95th
319 percentile range (2-sigma) of the same PDF. Posterior emissions and prior scaling maps are
320 shown in Fig. 5. A comparison of the atmospheric measurements with modelled mixing ratios is
321 shown in Fig. S1. For each gas, the sensitivity of the inversion to changes in the magnitude of the
322 prior is given in Fig. S2.

323

324 We estimated South African HCFC-22 emissions of 3.6 (1.3 – 8.7) Gg yr^{-1} in 2017. Our prior
325 scaling map (Fig. 5) suggests that the measurements at Cape Point provide sufficient information
326 for the inversion to adjust emissions from the entire country, as opposed to those exclusively
327 within close proximity to the measurement site. Despite this, our posterior estimate is somewhat
328 dependent on the choice of prior (Fig. S2), although for all but the smallest prior emissions field
329 (50% of the default), the resultant uncertainty range overlaps the mean of our original estimate.
330 As expected, the regions with large emissions typically corresponded with major urban areas,
331 most notably the city and surroundings of Johannesburg (approximate population of 4.4 million
332 in 2016).[46] The approximate correlation of emissions with population density is consistent with

333the use of HCFC-22 as a refrigerant in stationary air-conditioning units. Simmonds et al.[13]

334estimated global HCFC-22 emissions of 370.3 ± 45.9 Gg yr^{-1} in 2016. When placed in context to

335the global burden, South Africa's HCFC-22 emissions (~1% of the global total) are relatively

336small. Saikawa et al.[47] estimated combined African and Middle Eastern HCFC-22 emissions of

33736.4 ± 22.3 Gg yr^{-1} for 2009. Assuming that this total did not change significantly between 2009

338and 2017, South Africa could account for ~10% of HCFC-22 emissions from this region.

339Nevertheless, emissions from the African continent as a whole are comparatively small. As a

340comparison, Asian Annex 5 countries emitted 213 ± 20.8 Gg yr^{-1} in the same year.[47]

341

342
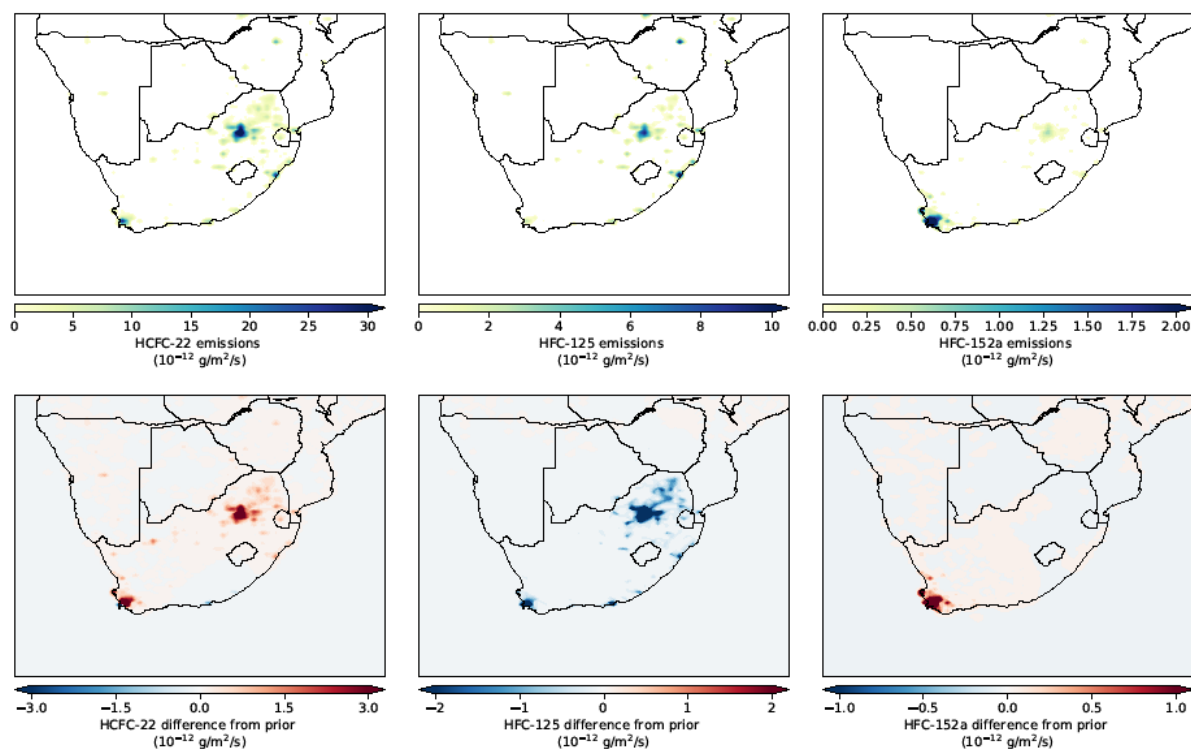
343**Figure 5.** Top) Maps of the posterior distribution of emissions of HCFC-22, HFC-125 and HFC-

344152a, based on measurements from the Cape Point monitoring station. Bottom) Maps of the

345difference between posterior and prior distributions of emissions, presented in the same units as

346above. Red indicates regions where the posterior was larger than the prior emissions field.

347   As consumption of HCFC-22 is reduced under the Montreal Protocol, it is widely expected

348that South Africa will accelerate the adoption of non-ozone depleting alternatives. R-410A (a

349zeotropic 50:50 blend of HFC-125 and HFC-32) is commonly cited as a replacement for HCFC-

35022 in refrigeration systems.[48] Our emission maps for these HCFC-22 and HFC-125 (Fig. 5)

351suggest a similar distribution of sources, with large emissions from Johannesburg and much

352smaller emissions from Cape Town. We estimate South Africa's HFC-125 emissions to be 1.6

353(0.8 – 2.6) Gg yr^{-1} in 2017. Simmonds et al.[49] estimated global HFC-125 emissions of 59.7 ± 9.5

354Gg yr^{-1} for 2015, hence South Africa represents approximately 2.7% of the global total. Unlike

355HCFC-22 and HFC-152a, our estimate for HFC-125 is insensitive to the choice of prior (Fig.

356S2), suggesting that the information content of the measurements is enough to provide some

357constraint for the whole of South Africa.

358   As with HFC-125, South Africa's emissions of HFC-152a might be expected to increase as it

359replaces ozone-depleting alternatives (e.g. HCFC-141b and HCFC-142b) in applications such as

360foam-blowing and as an aerosol propellant. We estimate South Africa's 2017 HFC-152a

361emissions to be 0.13 (0.10 – 0.19) Gg yr^{-1} which represent less than 0.4% of the global HFC-

362152a emissions estimated by Simmonds et al.[22] However, the model fit for this gas was poor,

363with a significant number of unresolved data points, possibly indicative of intermittent

364emissions, a strong local source or transport errors within NAME. These unresolved peaks also

365appear to hinder the ability of the inversion to adjust for emissions beyond Cape Town, though

366the posterior distribution is consistent with the HFC-152a bivariate plot in Fig. 4c, which

367suggests a single strong source to the north of Cape Point. The results of the sensitivity study

368show the inversion to be highly dependent on the choice of prior, consistent with the poor

369sensitivity of the inversion to distant sources. The uncertainty bounds for both small (50% of the

370default) and large (200% of the default) priors do not overlap with the mean original estimate.

371 The sensitivity of our HCFC-22 and HFC-152a emissions estimates to changes in the

372magnitude of the prior suggests that the inversion is insensitive to sources from the East of South

373Africa (e.g. those many hundreds of kilometres from Cape Point). To assess how robust our

374estimates are for sources near to the observatory (including Cape Town but excluding

375Johannesburg), a second set of emissions were estimated using the sub-domain shown in Fig. S3.

376The South West South Africa (SWSA) domain extends to a maximum latitude and longitude of

37730 °S and 24 °E, respectively. A summary of the results is shown in Fig. S4. Emissions of

378HCFC-22 and HFC-125 were very insensitive to the choice of prior. In contrast, HFC-152a

379remained sensitive to increases in the magnitude of the prior, suggesting that the presence of a

380persistent unresolvable signal results in a less robust estimate for this gas. We estimate SWSA

381emissions of 0.37 (0.20 – 0.55) Gg yr^{-1}, 0.10 (0.06 – 0.15) Gg yr^{-1} and 0.08 (0.07 – 0.09) Gg yr^{-1},

382accounting for 10%, 6% and 61% of South Africa's total emissions, for HCFC-22, HFC-125 and

383HFC-152a respectively.

384 As an Article-5 country, South Africa is not required to publish a detailed inventory of its

385greenhouse gas emissions.[14] Except for consumption statistics submitted as part of its Montreal

386Protocol commitments, South Africa's HCFC and HFC emissions are poorly defined. As per the

387HPMP, South Africa was required to freeze its HCFC consumption by 2013 (relative to a

3882009/10 baseline) followed by successive cuts leading to a complete phase-out by 2040. South

389Africa is also in the process of ratifying the Kigali Amendment to the Montreal Protocol, which

390sets out plans to reduce global emissions of HFCs and came into effect on January 1st 2019.

391However, South Africa will not be required to make its first reductions in the production or 392consumption of HFCs until 2040. Given the current and impending regulations imposed on 393South Africa's halocarbon emissions, in the absence of a nationwide monitoring programme for 394these compounds, plausible estimates of the country's emissions are useful. Ongoing 395atmospheric measurements of key HCFC and HFC mixing ratios at Cape Point provide a 396valuable means by which to verify South Africa's progress under the Kigali Amendment.

397   Further work is required to verify the results of this study, if these estimates are to form a 398reliable means of validation for future inventory work. Particular attention to better understand 399the local sources of HFC-152a is required, as it is possible that a strong source within close 400proximity of Cape Point could mask emissions from further afield. The usefulness of Cape Point 401as a means by which to estimate South Africa's halocarbon emissions is also likely to increase as 402the dataset grows. In particular, more data collected during the Southern Hemisphere autumn and 403winter months - which corresponds with a maximum in the sensitivity of the site to terrestrial 404sources – would be highly beneficial. In addition, further measurements from the East of the 405country and Johannesburg in particular would improve the ability of the inversion to accurately 406constrain sources from the entirety of South Africa.

407

408ASSOCIATED CONTENT

409Code availability

410   The inverse model code used in this study is available upon request from Matt Rigby 411(Matt.Rigby@bristol.ac.uk). The NAME model is available upon request to the UK Met Office.

₄₁₂AUTHOR INFORMATION

₄₁₃Corresponding author

₄₁₄*email: D.E.S. d.e.shallcross@bristol.ac.uk, Tel: +44 117 928 7796

₄₁₅Notes

₄₁₆The authors declare no competing financial interest.

₄₁₇

₄₁₈ACKNOWLEDGEMENTS

₄₂₄

₄₂₅REFERENCES

₄₂₆(1)   Derwent, R. G.; Volz-Thomas, A. The Tropospheric Lifetimes of Halocarbons and Their ₄₂₇   Reactions with OH Radicals: An Assessment Based on the Concentration of ^{14}CO. In

428   *UNEP/WMO Scientific Assessment of Stratospheric Ozone*; 1989; p Appendix.

429(2)   Liu, R.; Huie, R. E.; Kurylo, M. J. Rate Constants for the Reactions of the OH Radical

430   with Some Hydrochlorofluorocarbons over the Temperature Range 270-400 K.

431   *J.Phys.Chem.* **1990**, *94* (7), 3247–3249. https://doi.org/10.1021/j100371a004.

432(3)   Fisher, D. A.; Hales, C. H.; Filkin, D. L.; Ko, M. K. W.; Sze, N. D.; Connell, P. S.;

433   Wuebbles, D. J.; Isaksen, I. S. A.; Stordal, F. Model Calculations of the Relative Effects of

434   CFCs and Their Replacements on Stratospheric Ozone. *Nature* **1990**, *344* (6266), 508–

435   512. https://doi.org/10.1038/344508a0.

436(4)   Naik, V.; Jain, A. K.; Patten, K. O.; Wuebbles, D. J. Consistent Sets of Atmospheric

437   Lifetimes and Radiative Forcings on Climate for CFC Replacements: HCFCs and HFCs.

438   *J.   Geophys.   Res.   Atmos.*   **2000**,   *105*   (D5),   6903–6914.

439   https://doi.org/10.1029/1999JD901128.

440(5)   Velders, G. J. M. M.; Fahey, D. W.; Daniel, J. S.; McFarland, M.; Andersen, S. O. The

441   Large Contribution of Projected HFC Emissions to Future Climate Forcing. *Proc. Natl.*

442   *Acad.   Sci.   U.   S.   A.*   **2009**,   *106*   (27),   10949–10954.

443   https://doi.org/10.1073/pnas.0902817106.

444(6)   Papanastasiou, D. K.; Beltrone, A.; Marshall, P.; Burkholder, J. B. Global Warming

445   Potential Estimates for the $C_1 - C_3$ Hydrochlorofluorocarbons (HCFCs) Included in the

446   Kigali Amendment to the Montreal Protocol. *Atmos. Chem. Phys.* **2018**, *18*, 6317–6330.

447(7)   UNEP - Ozone Secretariat. *Amendement to the Montreal Protocol on Substances That*

448   *Deplete the Ozone Layer: Report*; Copenhagen, 1992.

449 (8) UNEP - Ozone Secretariat. *Amendment to the Montreal Protocol on Substances That*

450   *Deplete the Ozone Layer: Report*; Kigali, 2016.

451 (9) WMO. *Scientific Assessment of Ozone Depletion: 2014*; World Meteorological

452   Organization, 2014.

453 (10) Rinsland, C. P.; Chiou, L.; Boone, C.; Bernath, P.; Mahieu, E. First Measurements of the

454   HCFC-142b Trend from Atmospheric Chemistry Experiment (ACE) Solar Occultation

455   Spectra. *J. Quant. Spectrosc. Radiat. Transf.* **2009**, *110* (18), 2127–2134.

456   https://doi.org/10.1016/j.jqsrt.2009.05.011.

457 (11) Simmonds, P. G.; Rigby, M.; McCulloch, A.; O'Doherty, S. J.; Young, D.; Mühle, J.;

458   Krummel, P. B.; Steele, L. P.; Fraser, P. J.; Manning, A. J.; et al. Changing Trends and

459   Emissions of Hydrochlorofluorocarbons (HCFCs) and Their Hydrofluorocarbon (HFCs)

460   Replacements. *Atmos. Chem. Phys.* **2017**, *17* (7), 4641–4655. https://doi.org/10.5194/acp-

461   17-4641-2017.

462 (12) Burkholder, J. B.; Cox, R. A.; Ravishankara, A. R. Atmospheric Degradation of Ozone

463   Depleting Substances, Their Substitutes, and Related Species. *Chem. Rev.* **2015**, *115* (10),

464   3704–3759. https://doi.org/10.1021/cr5006759.

465 (13) Simmonds, P. G.; Rigby, M.; McCulloch, A.; Vollmer, M. K.; Henne, S.; Mühle, J.;

466   O'Doherty, S. J.; Manning, A. J.; Krummel, P. B.; Fraser, P. J.; et al. Recent Increases in

467   the Atmospheric Growth Rate and Emissions of HFC-23 (CHF_3) and the Link to HCFC-22

468   ($CHClF_2$) Production. *Atmos. Chem. Phys.* **2018**, *18* (6), 4153–4169.

469   https://doi.org/10.5194/acp-18-4153-2018.

470(14) Graziosi, F.; Arduini, J.; Furlani, F.; Giostra, U.; Kuijpers, L. J. M.; Montzka, S. A.; Miller,

471   B. R.; O'Doherty, S. J.; Stohl, A.; Bonasoni, P.; et al. European Emissions of HCFC-22

472   Based on Eleven Years of High Frequency Atmospheric Measurements and a Bayesian

473   Inversion   Method.   *Atmos.   Environ.*   **2015**,   *112*,   196–207.

474   https://doi.org/10.1016/j.atmosenv.2015.04.042.

475(15) Aucott, M. L.; McCulloch, A.; Graedel, T. E.; Kleiman, G.; Midgley, P.; Li, Y.-F.

476   Anthropogenic Emissions of Trichloromethane (Chloroform CHCl$_3$) and

477   Chlorodifluoromethane (HCFC-22): Reactive Chlorine Emissions Inventory. *J. Geophys.*

478   *Res.* **1999**, *104* (D7), 8405–8415. https://doi.org/10.1029/1999JD900053.

479(16) Xiang, B.; Patra, P. K.; Montzka, S. A.; Miller, S. M.; Elkins, J. W.; Moore, F. L.; Atlas, E.

480   L.; Miller, B. R.; Weiss, R. F.; Prinn, R. G.; et al. Global Emissions of Refrigerants HCFC-

481   22 and HFC-134a: Unforeseen Seasonal Contributions. *Proc. Natl. Acad. Sci.* **2014**, *111*

482   (49), 17379–17384. https://doi.org/10.1073/pnas.1417372111.

483(17) Forster, P.; Ramaswamy, V.; Artaxo, P.; Berntsen, T.; Betts, R.; Fahey, D. W.; Haywood, J.;

484   Lean, J.; Lowe, D. C.; Myhre, G.; et al. Climate Change 2007: The Physical Science

485   Basis. Contribution of Working Group I to the Fourth Assessment Report of the

486   Intergovernmental Panel on Climate Change. Chapter 2: Changes in Atmospheric and

487   Radiative   Forcing.   *Cambridge   Univ.   Press*   **2007**,   129–234.

488   https://doi.org/10.1103/PhysRevB.77.220407.

489(18) O'Doherty, S. J.; Miller, B. R.; Mühle, J.; McCulloch, A.; Simmonds, R. G.; Manning, A.

490   J.; Reimann, S.; Vollmer, M. K.; Greally, B. R.; Prinn, R. G.; et al. Global and Regional

491   Emissions of HFC-125 (CHF2CF3) from in Situ and Air Archive Atmospheric

492 Observations at AGAGE and SOGE Observatories. *J. Geophys. Res. Atmos.* **2009**, *114*

493 (23). https://doi.org/10.1029/2009JD012184.

494 (19) McCulloch, A. Evidence for Improvements in Containment of Fluorinated Hydrocarbons

495 during Use: An Analysis of Reported European Emissions. *Environ. Sci. Policy* **2009**, *12*

496 (2), 149–156. https://doi.org/10.1016/j.envsci.2008.12.003.

497 (20) Lunt, M. F.; Rigby, M.; Ganesan, A. L.; Manning, A. J.; Prinn, R. G.; O'Doherty, S.;

498 Mühle, J.; Harth, C. M.; Salameh, P. K.; Arnold, T.; et al. Reconciling Reported and

499 Unreported HFC Emissions with Atmospheric Observations. *Proc. Natl. Acad. Sci.* **2015**,

500 *112* (19), 5927–5931. https://doi.org/10.1073/pnas.1420247112.

501 (21) Li, P.; Mühle, J.; Montzka, S. A.; Oram, D. E.; Miller, B. R.; Tanhua, T. Global Annual

502 Mean Atmospheric Histories , Growth Rates and Seawater Solubility Estimations of the

503 Halogenated Compounds PFC-14 and PFC-116. *Ocean Sci. Discuss.* **2018**, No. August, 1–

504 51.

505 (22) Simmonds, P. G.; Rigby, M.; Manning, A. J.; Lunt, M. F.; O'Doherty, S. J.; McCulloch,

506 A.; Fraser, P. J.; Henne, S.; Vollmer, M. K.; Mühle, J.; et al. Global and Regional

507 Emissions Estimates of 1,1-Difluoroethane (HFC-152a, CH3CHF2) from in Situ and Air

508 Archive Observations. *Atmos. Chem. Phys.* **2016**, *16* (1), 365–382.

509 https://doi.org/10.5194/acp-16-365-2016.

510 (23) NEDLAC. *Hydrochlorofluorocarbons (HCFC) Phase Out Plan for South Africa*; National

511 Economic Development and Labour Council, Departmenet of Environmental Affairs:

512 Johannesburg, 2012.

513(24) Labuschagne, C.; Kuyper, B.; Brunke, E.; Spuy, D. Van Der; Martin, L.; Mbambalala, E.;

514   Khan, M. A. H.; Davies-coleman, M. T.; Shallcross, D. E.; Joubert, W. A Review of Four

515   Decades of Atmospheric Trace Gas Measurements at Cape Point, South Africa. *Trans. R.*

516   *Soc. South Africa* **2018**, 1–20. https://doi.org/10.1080/0035919X.2018.1477854.

517(25) Tyson, P. D.; Preston-Whyte, R. A. *The Weather and Climate of Southern Africa*; Oxford

518   University Press Southern Africa: Cape Town, 2000.

519(26) Preston-Whyte, R. A.; Tyson, P. D. *The Atmosphere and Weather of Southern Africa*;

520   Oxford University Press: Oxford, 1993.

521(27) Garstang, M.; Tyson, P. D.; Edwards, M.; Kallberg, P.; Lindesay, J. A. Horizontal and

522   Vertical Transport of Air over Southern Africa. *J. Geophys. Res.* **1996**, *101* (D19), 23721–

523   23736. https://doi.org/10.1029/95JD00844.

524(28) Brunke, E.; Walters, C.; Mkololo, T.; Martin, L. G.; Labuschagne, C.; Silwana, B.; Slemr,

525   F.; Weigelt, A.; Ebinghaus, R.; Somerset, V. Mercury in the Atmosphere and in Rainwater

526   at   Cape   Point,   South   Africa. *Atmos.   Environ.* **2016**, *125*, 24–32.

527   https://doi.org/10.1016/j.atmosenv.2015.10.059.

528(29) Simmonds, P. G.; O'Doherty, S. J.; Nickless, G.; Sturrock, G. A.; Swaby, R.; Knight, P.;

529   Ricketts, J.; Woffendin, G.; Smith, R. Automated Gas Chromatograph/Mass Spectrometer

530   for Routine Atmospheric Field Measurements of the CFC Replacement Compounds, the

531   Hydrofluorocarbons and Hydrochlorofluorocarbons. *Anal. Chem.* **1995**, *67* (4), 717–723.

532   https://doi.org/10.1021/ac00100a005.

533(30) O'Doherty, S. J.; Simmonds, P. G.; Nickless, G.; Betz, W. R. Evaluation of Carboxen

534   Carbon Molecular Sieves for Trapping Replacement Chlorofluorocarbons. *J. Chromatogr.*

535   **1993**, *630*, 265–274. https://doi.org/10.2989/02577619209504717.

536(31) Sturrock, G. A.; Porter, L. W.; Fraser, P. J. In Situ Measurement of CFC Replacement

537   Chemicals and Other Halocarbons at Cape Grim: The AGAGE GC-MS Program. In

538   *Baseline 97–98*; Tindale, N. W., Derek, N., Francey, R. J., Eds.; Bureau of Meteorology,

539   CSIRO: Melbourne, Victoria, 2001; pp 43–49.

540(32) Miller, B. R.; Weiss, R. F.; Salameh, P. K.; Tanhua, T.; Greally, B. R.; Mühle, J.;

541   Simmonds, P. G. Medusa: A Sample Preconcentration and GC-MS Detector System for in

542   Situ Measurements of Atmospheric Trace Halocarbons, Hydrocarbons and Sulfur

543   Compounds. *Anal. Chem.* **2008**, *80* (1), 1536–1545. https://doi.org/10.1021/ac702084k.

544(33) Arnold, T.; Mühle, J.; Salameh, P. K.; Harth, C. M.; Ivy, D. J.; Weiss, R. F. Automated

545   Measurement of Nitrogen Trifluoride in Ambient Air. *Anal. Chem.* **2012**, *84*, 4798–4804.

546   https://doi.org/10.1021/ac300373e.

547(34) O'Doherty, S. J.; Simmonds, P. G.; Cunnold, D. M.; Wang, H. J.; Sturrock, G. A.; Fraser,

548   P. J.; Ryall, D. B.; Derwent, R. G.; Weiss, R. F.; Salameh, P. K.; et al. In Situ Chloroform

549   Measurements at Advanced Global Atmospheric Gases Experiment Atmospheric Research

550   Stations from 1994 to 1998. *J. Geophys. Res. Atmos.* **2001**, *106* (D17), 20429–20444.

551   https://doi.org/10.1029/2000JD900792.

552(35) Manning, A. J.; O'Doherty, S. J.; Jones, A. R.; Simmonds, P. G.; Derwent, R. G.

553   Estimating UK Methane and Nitrous Oxide Emissions from 1990 to 2007 Using an

554   Inversion Modeling Approach. *J. Geophys. Res. Atmos.* **2011**, *116* (2), 1–19.

555   https://doi.org/10.1029/2010JD014763.

556(36) Lunt, M. F.; Rigby, M.; Ganesan, A. L.; Manning, A. J. Estimation of Trace Gas Fluxes

557   with Objectively Determined Basis Functions Using Reversible-Jump Markov Chain

558   Monte Carlo. *Geosci. Model Dev.* **2016**, *9* (9), 3213–3229. https://doi.org/10.5194/gmd-9-

559   3213-2016.

560(37) Ganesan, A. L.; Rigby, M.; Zammit-Mangion, A.; Manning, A. J.; Prinn, R. G.; Fraser, P.

561   J.; Harth, C. M.; Kim, K. R.; Krummel, P. B.; Li, S.; et al. Characterization of

562   Uncertainties in Atmospheric Trace Gas Inversions Using Hierarchical Bayesian Methods.

563   *Atmos. Chem. Phys.* **2014**, *14* (8), 3855–3864. https://doi.org/10.5194/acp-14-3855-2014.

564(38) Lunt, M. F.; Park, S.; Li, S.; Henne, S.; Manning, A. J.; Ganesan, A. L.; Simpson, I. J.;

565   Blake, D. R.; Liang, Q.; O'Doherty, S.; et al. Continued Emissions of the Ozone-

566   Depleting Substance Carbon Tetrachloride From Eastern Asia. *Geophys. Res. Lett.* **2018**,

567   *4*, 423–430. https://doi.org/10.1029/2018GL079500.

568(39) Say, D.; Ganesan, A. L.; O'Doherty, S.; Rigby, M.; Lunt, M. F.; Harth, C.; Manning, A. J.;

569   Krummel, P. B.; Bauguitte, S. J.-B. Atmospheric Observations and Emission Estimates of

570   Ozone-Depleting Chlorocarbons from India. *Atmos. Chem. Phys. Discuss.* **2018**.

571(40) Raupach, M. R.; Rayner, P. J.; Paget, M. Regional Variations in Spatial Structure of

572   Nightlights, Population Density and Fossil-Fuel CO2emissions. *Energy Policy* **2010**, *38*

573   (9), 4756–4764. https://doi.org/10.1016/j.enpol.2009.08.021.

574(41) Rigby, M.; Prinn, R. G.; O'Doherty, S. J.; Miller, B. R.; Ivy, D.; Mühle, J.; Harth, C. M.;

575   Salameh, P. K.; Arnold, T.; Weiss, R. F.; et al. Recent and Future Trends in Synthetic

576   Greenhouse Gas Radiative Forcing. *Geophys. Res. Lett.* **2014**, *41* (7), 2623–2630.

577   https://doi.org/10.1002/2013GL059099.

578(42) Rivett, A. C.; Martin, D.; Nickless, G.; Simmonds, P. G.; O'Doherty, S. J.; Gray, D. J.;

579   Shallcross, D. E. In Situ Gas Chromatographic Measurements of Halocarbons in an Urban

580   Environment. *Atmos. Environ.* **2003**, *37* (16), 2221–2235. https://doi.org/10.1016/S1352-

581   2310(03)00148-1.

582(43) Rivett, A. C.; Martin, D.; Gray, D. J.; Price, C. S.; Nickless, G.; Simmonds, P. G.;

583   O'Doherty, S. J.; Greally, B. R.; Knights, A.; Shallcross, D. E. The Role of Volatile

584   Organic Compounds in the Polluted Urban Atmosphere of Bristol, England. *Atmos. Chem.*

585   *Phys.* **2003**, *3* (4), 1165–1176. https://doi.org/10.5194/acp-3-1165-2003.

586(44) Mead, M. I.; Khan, M. A. H.; Bull, I. D.; White, I. R.; Nickless, G.; Shallcross, D. E.

587   Stable Carbon Isotope Analysis of Selected Halocarbons at Parts per Trillion

588   Concentration in an Urban Location. *Environ. Chem.* **2008**, *5* (5), 340–346.

589   https://doi.org/10.1071/EN08037.

590(45) Khan, M. A. H.; Mead, M. I.; White, I. R.; Golledge, B.; Nickless, G.; Knights, A.;

591   Martin, D.; Rivett, A. C.; Greally, B. R.; Shallcross, D. E. Year-Long Measurements of C_1-

592   C_3 Halocarbons at an Urban Site and Their Relationship with Meteorological Parameters.

593   *Atmos. Sci. Lett.* **2009**, *10*, 75–86. https://doi.org/10.1002/asl.

594(46) CIESEN. Gridded Population Of the World (gpw), V4.

595(47) Saikawa, E.; Rigby, M.; Prinn, R. G.; Montzka, S. A.; Miller, B. R.; Kuijpers, L. J. M.;

596   Fraser, P. J. B.; Vollmer, M. K.; Saito, T.; Yokouchi, Y.; et al. Global and Regional

597   Emission Estimates for HCFC-22. *Atmos. Chem. Phys.* **2012**, *12* (21), 10033–10050.

598   https://doi.org/10.5194/acp-12-10033-2012.

599 (48) Spatz, M. W.; Motta, S. F. Y. An Evalution of Options for Replacing HCFC-22 in Medium
600   Temperature Refrigeration Systems. *Int. J. Refrig.* **2004**, *27* (5), 475–483.
601   https://doi.org/10.1016/j.ijrefrig.2004.02.009.

602 (49) Simmonds, P. G.; Rigby, M.; McCulloch, A.; O'Doherty, S.; Young, D.; Mühle, J.;
603   Krummel, P. B.; Steele, P.; Fraser, P. J.; Manning, A. J.; et al. Changing Trends and
604   Emissions of Hydrochlorofluorocarbons (HCFCs) and Their Hydrofluorocarbon (HFCs)
605   Replacements. *Atmos. Chem. Phys.* **2017**, *17* (7), 4641–4655. https://doi.org/10.5194/acp-
606   17-4641-2017.

607

608

609

610

611

612

613 SUPPLEMENTARY INFORMATION

## 614 S1 Baseline classification algorithm

615 The baseline classification algorithm uses a three-step process to determine a baseline fit. A
616 121-day rolling window, consisting of measurements for 60 days either side of each sampling
617 day was used in the baseline fit. In the first step the daily minima over the whole 121-day

618window were determined. A second order polynomial was then fitted to the daily minima. The

619polynomial fit was subtracted from each measurement in the 121-day window, creating a matrix

620of distances from the polynomial fit. The median of the distances was calculated, which has been

621shown to be less sensitive to outliers compared to the mean.[34] Only distance values below the

622median were used in the variability calculation. The variability of the distance matrix was

623determined by the root mean square (RMS) deviation (σ) of the distances. Values in the distance

624dataset larger than 3σ (tunable) above the median were marked as 'polluted'. Consequently, all

625the other values were marked as baseline. Only the marked data ('pollution' and 'baseline') for

626the day of the event were retained and the window moved to the next sampling day.

627 The baseline fit was improved in the second step, which was identical to the first step,

628described above, except that the data marked as 'polluted' were excluded. The repeat of the

629procedure without the 'polluted' marked data is important especially for highly polluted air, as

630extremely elevated observations can bias the median. Measurements that were between 2σ and

631$3\sigma$ in this second round were marked as 'possibly polluted'.

632 The third step analysed the data marked as 'possibly polluted'. A test was performed to

633examine if a point marked as 'possibly polluted' was adjacent to 'polluted' data point. If there

634was adjacency, then the 'possibly polluted' data point was reclassified as 'polluted'. If

635measurements were not marked as polluted these were then considered as baseline.

636

637
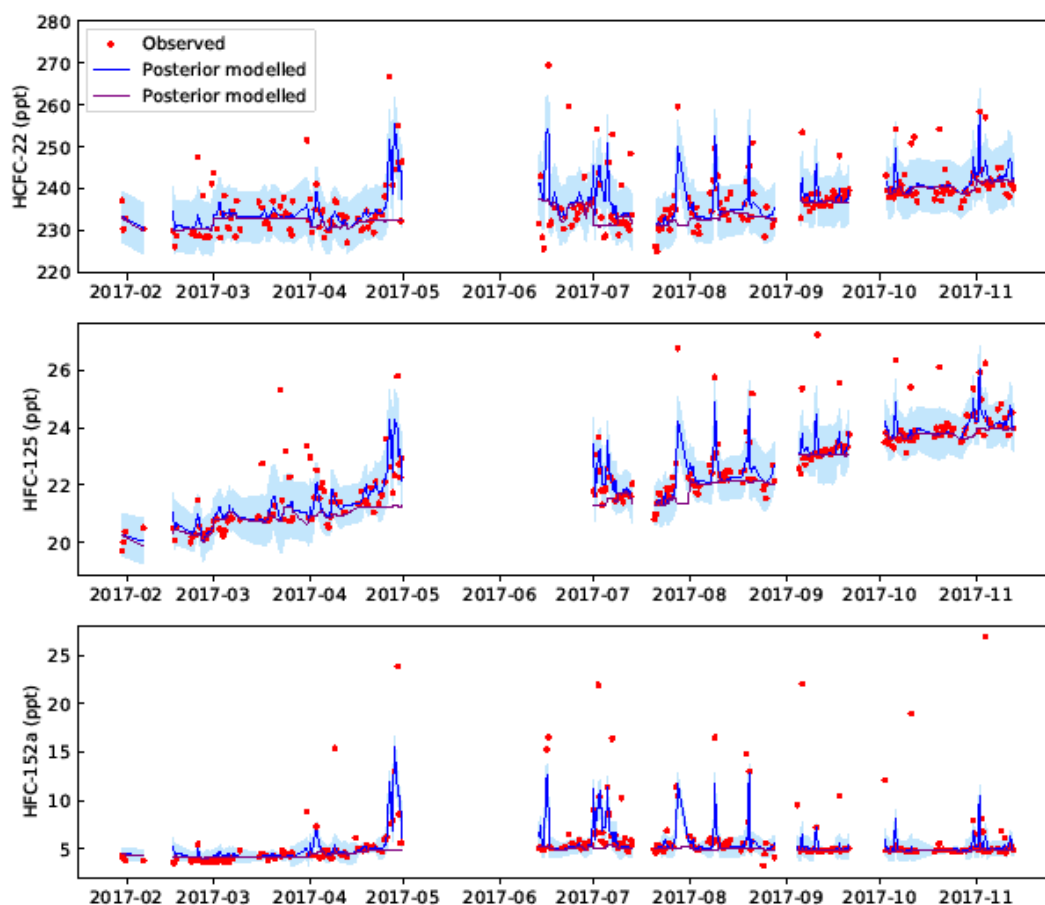
Figure S1: A comparison of measured (red points, ppt) and modelled (blue line, ppt) mole
fractions at Cape Point. Observations and NAME back-trajectories were binned into 12-hour
averages. Model uncertainty (95th percentile confidence interval) is represented by the pale blue
shading. The modelled baseline (purple line) is also shown.

643
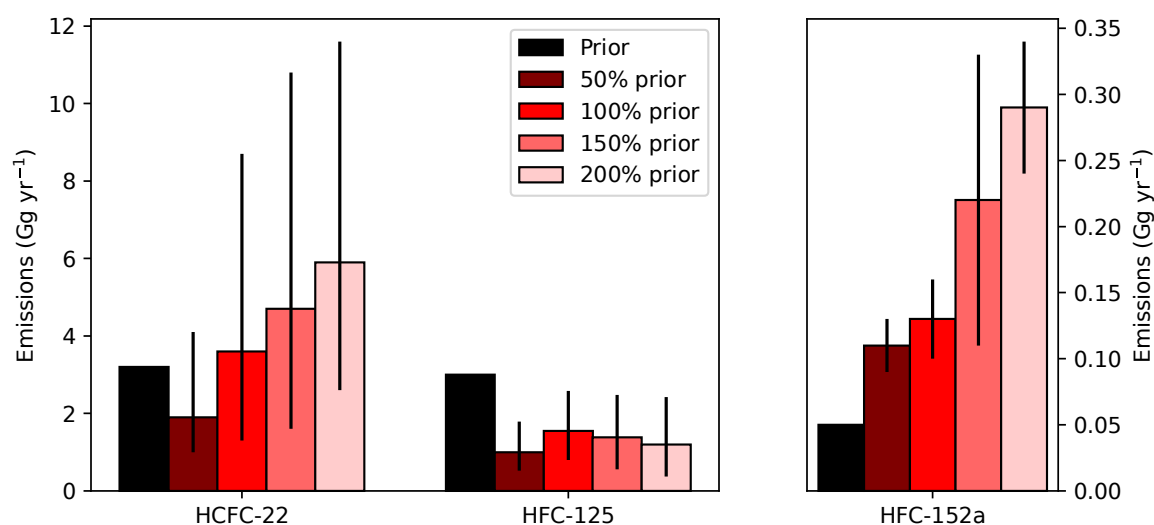
Figure S2: Sensitivity plots showing the change in posterior emissions as a result of scaling
(50% - 200%) of the prior. Error bars represent the 95th percentile confidence interval of the
posterior PDFs.

647

648
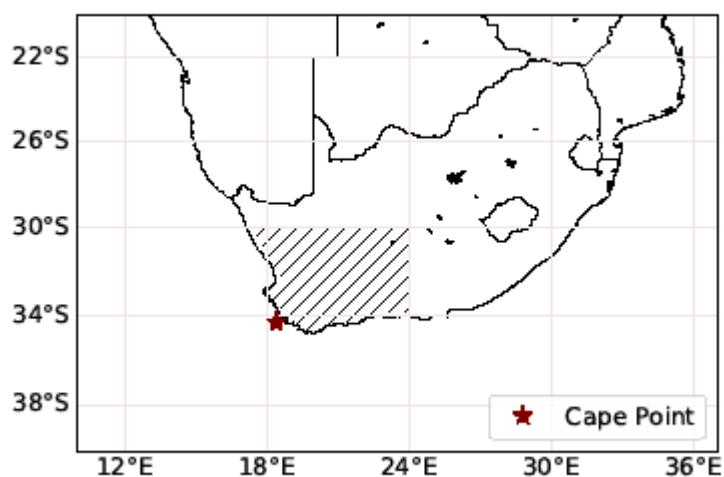
Figure S3: Plot showing the reduced domain for South West South Africa (SWSA, hatched
lines). The Cape Point observatory is also shown (red star).

651

652
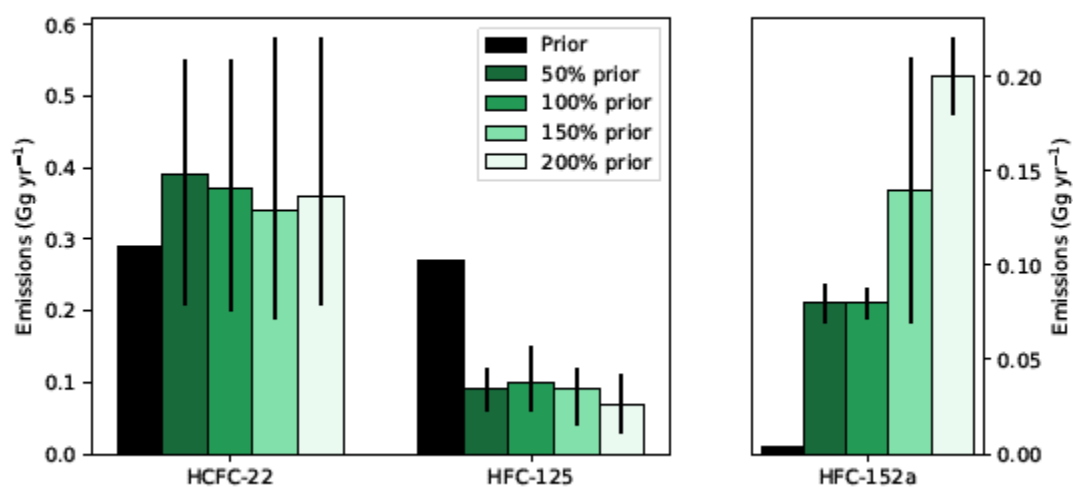
Figure S4: Sensitivity plots showing the change in posterior emissions for the reduced South West South Africa domain as a result of scaling (50% - 200%) of the prior. Error bars represent the 95th percentile confidence interval of the posterior PDFs.

656

657

658